

# The thermal expansion of carbon fibre-reinforced plastics

## Part 2 *The influence of fibre volume fraction*

B. YATES, M. J. OVERY,\* J. P. SARGENT, B. A. McCALLA  
*Department of Pure and Applied Physics, University of Salford, UK*

D. M. KINGSTON-LEE, L. N. PHILLIPS, K. F. ROGERS  
*Materials Department, Royal Aircraft Establishment, Farnborough, UK*

Interferometric measurements of the linear thermal expansion coefficients of epoxy resin DLS 351/BF<sub>3</sub> 400 are reported over the approximate temperature range 90 to 500 K. Corresponding measurements in directions parallel and perpendicular to the fibres are also reported for unidirectional composite bars of Courtaulds HTS carbon fibre in this resin, at nominal fibre volume contents of 50, 60 and 80%. The results are qualitatively similar to earlier observations upon resin ERLA 4617/mPDA-based specimens, but effects associated with resin softening occur at significantly higher temperatures in the case of resin DLS 351/BF<sub>3</sub> 400. Current theoretical models account successfully for the influence of fibre volume fraction in the range 0.5 to 0.8 upon the value of the coefficient of thermal expansion at room temperature, within the limitations imposed by experimental uncertainty, provided that appropriate values are assigned to the linear thermal expansion coefficients of the fibres. In the directions parallel ( $\alpha_{\parallel}^f$ ) and perpendicular ( $\alpha_{\perp}^f$ ) to the fibre axis these values have been selected from the ranges  $-10 \times 10^{-7} < \alpha_{\parallel}^f < -9 \times 10^{-7}$  and  $0.5 \times 10^{-5} < \alpha_{\perp}^f < 1.9 \times 10^{-5}$ . It is concluded that a more rigorous appraisal must await the availability of independent information concerning the directional thermoelastic properties of carbon fibres.

### 1. Introduction

In the preceding paper [1] in this series (henceforth referred to as Part 1), a description of the background to a series of experimental investigations of the thermal expansion characteristics of carbon fibre-reinforced plastics bars was followed by an account of measurements in which particular attention was paid to the influence of fibre type and orientation. Both unidirectional and bidirectional arrays of fibres in a single epoxy resin, ERLA 4617/mPDA were examined.

A further factor of prime importance in studies of the thermal expansions of these materials is the fibre volume fraction. An examination of the

influence of this parameter was therefore included in the programme and the account which follows contains a description of the measurements and the extent to which they may be understood in terms of current theoretical models.

### 2. The specimens and their investigation

For the present purpose one epoxy resin matrix was selected, together with three nominal fibre volume fractions, 50, 60 and 80%, the first two being commonly employed in commercial applications. The epoxy resin is designated by the manufacturer† DLS 300 or DLS 351, depending upon whether it is obtained in the form of a

\*Present address: Walthamstow Hall, Sevenoaks, Kent, UK

†Ciba-Geigy Ltd, Cambridge, UK

TABLE I The specimens

Bar number	Specimen designation	Description	Direction of thermal expansion measurements	Fibre volume (%)	Void content (%)
8	18	Pure resin		0.0	0.0
9	19	Unidirectional	Parallel to fibres	51.5	2.2
9	20	Unidirectional	Perpendicular to fibres	51.5	2.2
10	21	Unidirectional	Parallel to fibres	60.7	1.6
10	22	Unidirectional	Perpendicular to fibres	60.7	1.6
11	23	Unidirectional	Parallel to fibres	78.9	2.8
11	24	Unidirectional	Perpendicular to fibres	78.9	2.8

solution with included  $\text{BF}_3400$  hardener or in solid form without hardener. Descriptions of the bars and the specimens prepared from them are contained in Table I, in which the designations follow sequentially from those of Part 1.

The cast resin bar, bar 8, was made from DLS 351 hardened with Shell Epikure  $\text{BF}_3400$ . 1.2g  $\text{BF}_3400$  were dissolved in 80g DLS 351 at  $100^\circ\text{C}$ ; the resin was then out-gassed in a vacuum oven for 30 min, poured into a steel bar-mould and out-gassed at  $100^\circ\text{C}$  for a further 15 min. The vacuum was released and the resin maintained at  $100^\circ\text{C}$  for a further 15 min to give a total pre-cure time of 2 h. The temperature of the mould was then raised to  $150^\circ\text{C}$  over

30 min and maintained at  $150^\circ\text{C}$  for 2 h. The resin was finally post-cured at  $190^\circ\text{C}$  for 15 h, yielding a void-free bar containing a small proportion of specks of foreign matter.

Bars 9, 10 and 11 were prepared from aligned tows by the technique described earlier [1, 2], using the above curing cycle. Bars 10 and 11 were prepared from DLS 351 hardened with  $\text{BF}_3400$ ; Bar 9, which was produced earlier in the series, was prepared from DLS 300. There is no reason to expect the structure or physical properties of the cured resins to differ significantly; for this reason the single term DLS 351 will be used when making future reference to all specimens in this series. Courtaulds high strength surface treated (HTS)

TABLE II Smoothed values of the linear thermal expansion coefficients  $\alpha$  of the specimens described in Table I

$T$ (K)	$\alpha$ for the specimens numbered below ( $\text{K}^{-1}$ )						
	18	19	20	21	22	23	24
	( $\times 10^{-5}$ )	( $\times 10^{-7}$ )	( $\times 10^{-5}$ )	( $\times 10^{-7}$ )	( $\times 10^{-5}$ )	( $\times 10^{-7}$ )	( $\times 10^{-5}$ )
90	2.33	-1.8	1.57	-5.3	1.40	-4.1	1.00
100	2.46	-2.2	1.67	-6.1	1.49	-4.4	1.05
120	2.73	-2.7	1.86	-7.0	1.65	-5.0	1.16
140	3.00	-2.9	2.05	-7.5	1.81	-5.7	1.26
160	3.25	-3.1	2.21	-7.5	1.97	-6.5	1.35
180	3.50	-3.0	2.37	-7.1	2.12	-7.1	1.44
200	3.76	-2.9	2.51	-6.2	2.24	-7.4	1.52
220	4.00	-2.6	2.65	-5.0	2.35	-7.4	1.60
240	4.25	-2.2	2.77	-3.5	2.46	-7.2	1.66
260	4.48	-1.8	2.87	-2.5	2.55	-6.9	1.72
280	4.70	-1.2	2.95	-2.0	2.63	-6.4	1.77
300	4.80	-0.5	3.01	-2.0	2.66	-5.7	1.80
320	4.93	0.2	3.05	-4.2	2.71	-5.6	1.83
340	5.10	0.9	3.13	-4.6	2.78	-5.9	1.84
360	5.34	1.4	3.27	-3.0	2.87	-5.8	1.90
380	5.60	1.9	3.49	-0.4	2.98	-5.2	1.99
400	5.90	2.2	3.78	1.5	3.15	-3.5	2.13
420	6.25	2.4	4.13	1.9	3.35	-2.4	2.33
440	6.60	2.4	4.52	1.3	3.61	-1.8	2.61
460	7.02	2.0	4.95	0.2	3.94	-1.6	3.00
480	7.58	0.9	5.43	-1.5	4.39	-2.1	3.63
500	8.25	-1.3		-4.4	5.06		
510	8.68	-3.0		-8.0			
520	9.35	-5.5					

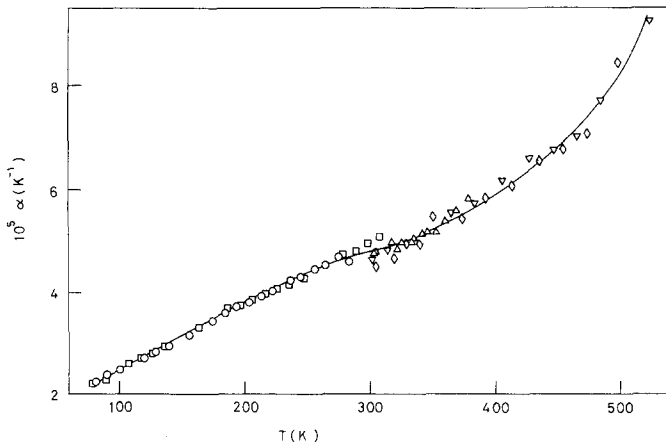


Figure 1 The linear thermal expansion coefficient  $\alpha$  of specimens 20:  $\circ$  run 1,  $\square$  run 2,  $\triangle$  run 3,  $\nabla$  run 4,  $\diamond$  run 5.

carbon fibre Batch PT 112/21 Z was used throughout. Sets of three specimens for interferometry were prepared from the bars in the manner described in Part 1, which also includes a description of the apparatus and the experimental procedure.

### 3. Results

Table II contains smoothed data for technological and analytical applications, corresponding to the primary data which are plotted in Figs. 1 to 7. The principal features of these temperature dependences qualitatively resemble those previously seen in the corresponding cases of the ERLA 4617/*m*PD A-matrix specimens. The predominant roles of the resin and fibre in particular directions within individual specimens and particular temperature ranges also appear to correspond. Of more interest are the differences between results for corresponding specimens containing a nominally common fibre type, concentration and orientation but in different resins, and the effects of fibre volume content.

It may be noted that marked signs of the influence of resin softening upon the thermal expansion of resin DLS 351, displayed in Figs 1 to 7, occur at significantly higher temperatures than in the corresponding specimens based upon resin ERLA 4617/*m*PD A and described in Part 1. This renders resin DLS 351 particularly suitable for the present purpose, since most theoretical models describing the thermoelastic behaviour of composites assume that the constituents of the composite are elastic. In the case of specimens based upon DLS 351 this is certainly true at ambient temperature, which is the only temperature at which the elastic constants of the resin (and approximate values for the elastic constants

of the fibre) are known. Compliance with this elasticity criterion was not quite as definite in the case of the specimens based upon resin ERLA 4617/*m*PD A, since it softened at a lower temperature.

A second comparative observation is afforded by a study of the results for specimens 18, 19, 21 and 23 displayed in Figs. 1, 2, 4 and 6. In the temperature region at which resin softening occurred the coefficient of thermal expansion in the direction parallel to the fibres varied inversely with the proportion of fibres, as might be expected. Below room temperature, however, although the results became more negative as the fibre volume fraction increased from 51.5 to 60.7%, a further increase to 78.9% produced no further significant change. This constancy may be due to a breakdown in the micro-mechanics because of effects associated with the presence of voids and an imperfect distribution of fibres. At these low temperatures the results are not as negative as corresponding results for pyrolytic graphite [3], presumably because of the poorer alignment of the direction perpendicular to the *c*-axes of the crystallites of the fibres with the direction of measurement.

A further comparative observation may be made upon the results for specimens 18, 21 and

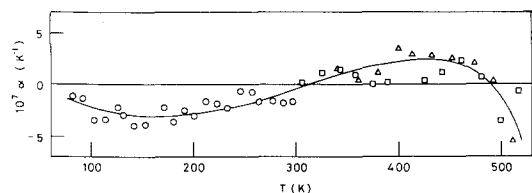


Figure 2 The linear thermal expansion coefficient  $\alpha$  of specimens 19:  $\circ$  run 1,  $\square$  run 2,  $\triangle$  run 3.

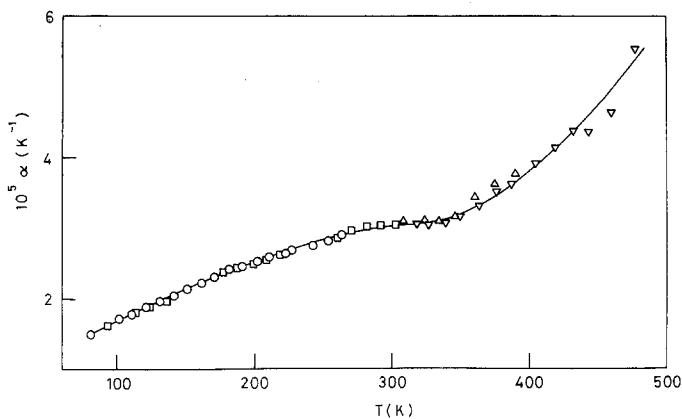


Figure 3 The linear thermal expansion coefficient  $\alpha$  of specimens 20:  $\circ$  run 1,  $\square$  run 2,  $\triangle$  run 3,  $\nabla$  run 4.

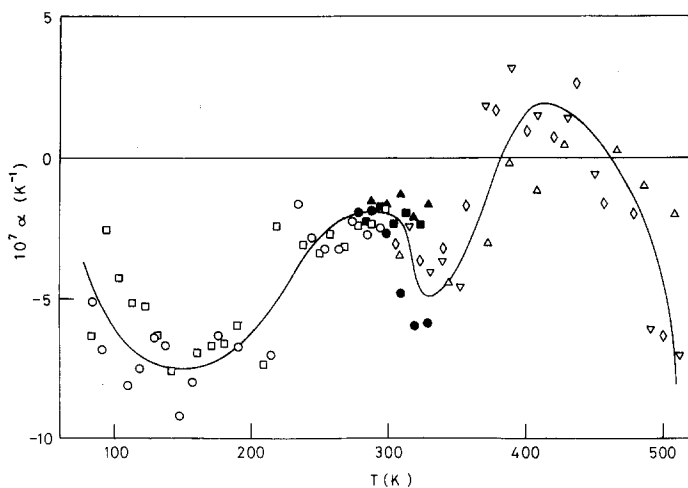


Figure 4 The linear thermal expansion coefficient  $\alpha$  of specimens 21:  $\circ$  run 1,  $\square$  run 2,  $\triangle$  run 3,  $\nabla$  run 4,  $\diamond$  run 5,  $\bullet$  run 6,  $\blacksquare$  run 7,  $\blacktriangle$  run 8.

23, in which irregularities are apparent in the temperature dependences of the thermal expansions in the region of ambient temperature. The existence of this discontinuous behaviour is almost masked by the experimental uncertainties in Fig. 1 and its presence was not fully appreciated before undertaking the measurements on specimens 21. From the sequence illustrated in Fig. 4 it may be discerned that the specimens were transferred from one of the two sets of apparatus (described in Part 1) to the other between runs 2 and 3, and that the discontinuity coincided approximately with the temperature of the changeover. In order to ensure that the effect was not due to the instrumentation, the linear thermal expansion coefficients of NBS silica test specimens, detailed results for which were reported in Part 1, were re-measured in both sets of apparatus in turn, following run 5. From the favourable agreement of these results with data supplied by the National Bureau of Standards it was concluded that the discontinuity observed

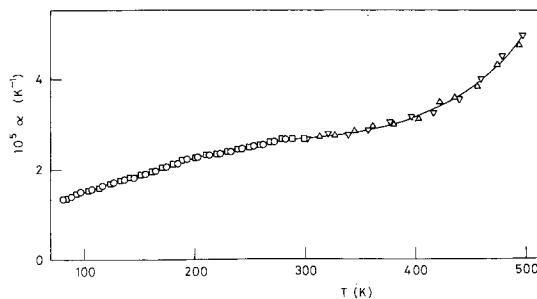


Figure 5 The linear thermal expansion coefficient  $\alpha$  of specimens 22:  $\circ$  run 1,  $\square$  run 2,  $\triangle$  run 3,  $\nabla$  run 4.

in the results for specimens 21 was real. In order to provide further confirmation specimens 21 were mounted in the low temperature apparatus again and three more completely separate sets of measurements were undertaken in the neighbourhood of the high temperature limit of this apparatus, in order to overlap the earlier results obtained in the high temperature apparatus. A similar discontinuity appeared when specimens 23 were investigated, and additional confirmation

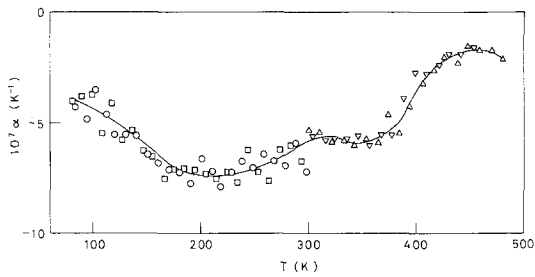


Figure 6 The linear thermal expansion coefficient  $\alpha$  of specimens 23:  $\circ$  run 1,  $\square$  run 2,  $\triangle$  run 3,  $\nabla$  run 4.

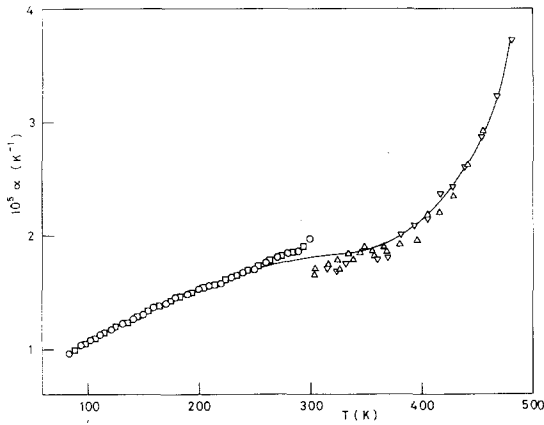


Figure 7 The linear thermal expansion coefficient  $\alpha$  of specimens 24:  $\circ$  run 1,  $\square$  run 2, (specimens A);  $\triangle$  run 3,  $\nabla$  run 4, (specimens B).

of the physical origin of the observations was provided by completely independent differential calorimetric investigations conducted upon the pure resin, the results of which displayed corresponding effects at comparable temperatures.

The results displayed in Figs. 3, 5 and 7, corresponding to the direction perpendicular to the fibre axes, fall into place within a sequence which includes the results for the pure resin (Fig. 1). The results for specimens 24, which contained the highest volume fraction of fibre, were significantly lower than corresponding results for pyrolytic graphite in the  $c$ -direction at all but the highest temperatures [3, 4], presumably because of the distribution of the  $c$ -axes of the crystallites about the fibre axis. The first set of specimens 24, (set A), was unfortunately purloined after the investigation below room temperature, and a second set (set B) was prepared for measurement above room temperature. The smoothed results tabulated for these specimens mask a discontinuity observed in the

neighbourhood of 300 K. Time has prevented a search for its cause, but it is hoped to examine this, along with other secondary effects, in a future investigation.

#### 4. Discussion

The majority of attempts to explain the thermal expansion behaviour of composites in terms of the thermal expansion coefficients and elastic constants of the constituents have been developed in terms of particulate reinforcement, in which homogeneous and isotropic constituents have been assumed to be distributed uniformly, producing composites which are macroscopically homogeneous and isotropic [5–12]. These models have enjoyed varying degrees of success, but the general comment may be made that satisfactory explanations of the detailed influence of particle size, shape and agglomeration have yet to be provided.

The problems posed by unidirectional fibrous composites, in which the constituents are homogeneous and isotropic, have been tackled by modifying equations emerging from the foregoing treatments of the particulate case and also by adopting completely independent approaches. Prominent among these is the model due to Schapery [13], who employed complementary and potential energy principles of thermoelasticity theory in conjunction with a procedure for minimizing the difference between upper and lower bounds. It was shown that in some important cases, two of which resemble those corresponding to the subjects of the present investigation, the bounds coincided and yielded exact solutions. In common with earlier models, the modified equation for the linear thermal expansion coefficient of the composite in a direction parallel to the carbon fibres reduces to the simple rule of mixtures.

$$\alpha_{11}^c = \frac{E_m \alpha_m V_m + E_{\parallel}^f \alpha_{\parallel}^f V_f}{E_m V_m + E_{\parallel}^f V_f} \quad (1)$$

provided that the Poisson's ratios of the matrix and fibres are closely similar. In this equation  $\alpha_m$ ,  $\alpha_{\parallel}^f$  are the linear thermal expansion coefficients and  $E_m$ ,  $E_{\parallel}^f$  the Young's moduli respectively of the matrix and of the fibres in the direction parallel to their length, and  $V_m$ ,  $V_f$  are the volume fractions of matrix and fibres. The Young's modulus and Poisson's ratio of DLS 351 were

taken as  $4.90 \text{ GN m}^{-2}$  and  $0.35$  respectively [14],  $E_{\parallel}^f$  was taken as  $262 \text{ GN m}^{-2}$  and  $\alpha_{\parallel}^f$  was adjusted to give the best fit to the experimental results, producing the results displayed in Fig. 8. The value of  $\alpha_{\parallel}^f$  emerging from this fitting process was  $-9.0 \times 10^{-7} \text{ K}^{-1}$ , which compares favourably with the value  $-9.1 \times 10^{-7} \text{ K}^{-1}$  deduced by Pirgon *et al.* [2] from their investigations of ERLA 4617/*m*PDA-based composite specimens. For the reasons discussed at some length in Part 1, it is difficult to assess uncertainty limits for the experimental results. There can be no doubt however that these will more than account for the differences between the experimental data and the smooth curve.

For the transverse direction of a unidirectional composite containing isotropic fibres of linear thermal expansion coefficient  $\alpha_f$  and Poisson's ratio  $\nu_f$  Schapery went on to produce the expression

$$\alpha_{22}^c = (1 + \nu_m)\alpha_m V_m + (1 + \nu_f)\alpha_f V_f - \alpha_{11}^c \nu_c \quad (2)$$

in which  $\nu_m$  is the Poisson's ratio of the matrix and  $\nu_c$  that of the composite. Although a rigorous application of Schapery's approach to the case of a composite containing anisotropic fibres lies outside the scope of the present investigation, the results given by an approximation produced by a simple adaptation of Equation 2 are compared with the experimental results at room temperature in Fig. 9. In this fitting process the linear thermal expansion coefficient of a fibre in a direction perpendicular to its length,  $\alpha_{\perp}^f$ , was taken to be  $0.5 \times 10^{-5} \text{ K}^{-1}$  in order to obtain the agreement shown.

Another consideration of the same system was made by Schneider [15], who assumed a hexagonal arrangement of cylindrical fibre/matrix elements, each element consisting of a fibre surrounded by a cylindrical matrix jacket. The matrix wedges between the elements were ignored initially but later included. Schneider's treatment was also restricted to the case of isotropic phases; the adapted version of his equation for  $\alpha_{11}^c$  again took the form of Equation 1. For the transverse direction he derived the equation

$$\alpha_{22}^c = \alpha_m - (\alpha_m - \alpha_f) \left[ \frac{2(1 + \nu_m)(\nu_m^2 - 1)C}{(1 + 1.1V_f)/(1.1V_f - 1) - \nu_m + 2\nu_m^2 C} - \frac{\nu_m E_f/E_m}{1/C + E_f/E_m} \right] \quad (3)$$

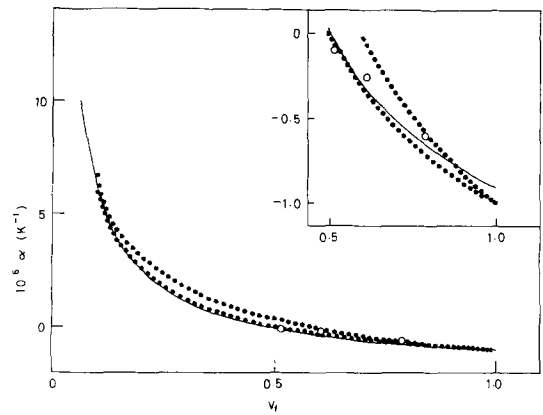


Figure 8 The linear thermal expansion coefficient  $\alpha$  of specimens 19, 21, 23 at ambient temperature, compared with theoretical predictions over a range of fibre volume fraction  $V_f$ :  $\circ$  smoothed experimental results; — curve corresponding to Equation 1 assuming  $\alpha_{\parallel}^f = -9.0 \times 10^{-7} \text{ K}^{-1}$ ;  $\bullet\bullet\bullet$  upper and lower bounds corresponding to the model of Das Gupta [18] assuming  $\alpha_{\parallel}^f = -9.7 \times 10^{-7} \text{ K}^{-1}$ .

in which  $C = 1.1 V_f / (1 - 1.1 V_f)$  and the other terms have their usual meanings. Although the derivation of this equation contains a number of approximations, reference to Fig. 9 shows that it fits the experimental data remarkably well when a value of  $\alpha_{\perp}^f = 1.4 \times 10^{-5} \text{ K}^{-1}$  is assumed.

Adapting equations corresponding to a more general system developed by Rosen and Hashin [16], Rosen [17] has examined the special case of isotropic fibrous inclusions in an isotropic matrix. It was found that for this particular symmetry the bounds of this model reduced to those of Schapery and that for the special case of a two-phase composite the bounds coincided. A characteristic feature of the results given by Schapery [13], Schneider [15] and Rosen [17] is the presence of a maximum in the transverse linear thermal expansion coefficient of a two-phase composite consisting of a high modulus fibre contained in a low modulus matrix, at a low fibre volume fraction.

The completely general case of the linear thermal expansion coefficients of an anisotropic

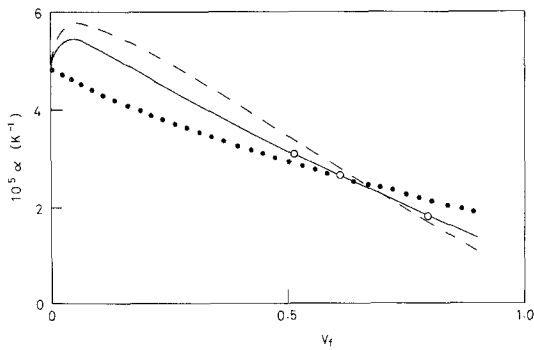


Figure 9 The linear thermal expansion coefficient  $\alpha$  of specimens 20, 22, 24 at ambient temperature, compared with theoretical predictions over a range of fibre volume  $V_f$ :  $\circ$  smoothed experimental results. Curves corresponding to theoretical models: --- Schapery [13]; ——— Schneider [14];  $\bullet\bullet\bullet$  Chamberlain (hexagonal packing) [17].

composite consisting of anisotropic constituents has been dealt with in a formal way in a treatment mentioned above [16]. The particular forms taken by the complex algebraic expressions corresponding to constituents having symmetries resembling those of the subjects of the present study are not readily available, however, and more immediate appraisals are possible with the aid of alternative models. Particular mention may be made of that due to Chamberlain [18], who dealt specifically with the case of carbon fibres embedded in a resin matrix and to whose work reference was made in Part 1. In this approach the compatibility of strains between fibres and matrix was satisfied on the basis that the net load in the fibre direction was zero. The total net strain was then related to the linear thermal expansion coefficient in this direction. For the transverse direction a circular section fibre rod surrounded by matrix material in the form of a thick-walled cylinder was considered, in which the radial displacements on the outside of the cylinder were related to the expansion coefficients in the transverse direction. Chamberlain's equation for  $\alpha_{11}^c$  is also given by Equation 1; his equation for the transverse direction, quoted in Part 1, is

$$\alpha_{22}^c = \alpha_m + \frac{2(\alpha_{11}^f - \alpha_m)V_f}{\nu_m(F - 1 + V_m) + (F + V_f) + \frac{E_m}{E_{11}^f}(1 - \nu_{11}^f)(F - 1 + V_m)} \quad (4)$$

in which  $F = 0.9096$  for hexagonal packing of the fibres and  $0.7854$  for square packing. An indication of the extent to which this equation provides a satisfactory representation of the experimental results is contained in Fig. 9, in the calculation of which  $\alpha_{11}^f$  was taken as  $1.9 \times 10^{-5} \text{ K}^{-1}$ . Mention may also be made of a model due to Das Gupta [19], who applied extremum principles of thermoelasticity to derive bounds on the linear thermal expansion coefficients in the direction of the fibre axes of unidirectional composite materials constructed from anisotropic phases. Some idea of the extent to which this model satisfactorily accounts for the appropriate experimental data may be gained from Fig. 8, in which a value of  $\alpha_{11}^f = -9.7 \times 10^{-7} \text{ K}^{-1}$  has been assumed in order to achieve the agreement shown.

## 5. Conclusions

In view of the uncertainties in some of the numerical data adopted in this assessment of current theoretical models, together with the experimental uncertainties in the measurements, undue significance should not be attached to the relative degrees of agreement between the predictions and the experimental results. All the models contain assumptions and approximations, and in the absence of precise knowledge of the thermoelastic properties of the carbon fibres themselves, a more rigorous appraisal would be premature. Within the limitations contained by the models, the experimental data examined here and previously [2] are consistent with the fibres having, at room temperature, linear thermal expansion coefficients,  $-10 \times 10^{-7} \text{ K}^{-1} < \alpha_{11}^f < -9 \times 10^{-7} \text{ K}^{-1}$  in the direction parallel and  $0.5 \times 10^{-5} \text{ K}^{-1} < \alpha_{11}^f < 1.9 \times 10^{-5} \text{ K}^{-1}$  in the direction perpendicular to their length. In the absence of more direct information, further evidence validating these conclusions might be sought by extending investigations to cover significantly lower fibre volume fractions, provided that a uniform dispersion of fibres could be achieved at such levels and that truly representative specimens could be prepared.

## Acknowledgement

We wish to express our gratitude to Dr J. Batchelor of The Railway Technical Centre, Derby, for the determination of the Young's modulus and Poisson's ratio of the resin, and to Dr S. Das Gupta of Bell Telephone Laboratories, Columbus, for helpful correspondence. The work described in this paper was performed under contract to the Ministry of Defence (Procurement Executive), to whom three of the authors (MJO, JPS and BAM) are grateful for financial support.

## References

1. K. F. ROGERS, L. N. PHILLIPS, D. M. KINGSTON-LEE, B. YATES, M. J. OVERY, J. P. SARGENT and B. A. MCCALLA, *J. Mater. Sci.* **12** (1977) 718.
2. O. PIRGON, G. H. WOSTENHOLM and B. YATES, *J. Phys. D: Appl. Phys.* **6** (1973) 309.
3. A. C. BAILEY and B. YATES, *J. Appl. Phys.* **41** (1970) 5088.
4. B. T. KELLY, B. YATES and O. PIRGON, Proceedings of the Fourth SCI Conference on Industrial Carbons and Graphite, London, 1974 (to be published).
5. P. S. TURNER, *J. Res. Nat. Bur. Stand.* **37** (1946) 239.
6. E. H. KERNER, *Proc. Phys. Soc.* **B69** (1956) 808.
7. G. ARTHUR and J. A. COULSON, *J. Nuclear Mater.* **13** (1964) 242.
8. T. J. HUGHES and J. O. BRITAIN, *Phys. Rev.* **135** (1964) A 1738.
9. J. L. CRIBB, *Nature* **220** (1968) 576.
10. T. T. WANG and T. K. KWEI, *J. Polymer Sci.* **A27** (1969) 889.
11. A. A. FAHMY and A. N. RAGAI, *J. Appl. Phys.* **41** (1970) 5108.
12. R. R. TUMMALA and A. L. FRIEDBERG, *ibid* **41** (1970) 5104.
13. R. A. SCHAPERY, *J. Comp. Mater.* **2** (1968) 380.
14. J. BATCHELOR, private communication.
15. W. SCHNEIDER, *Kunststoffe* **61** (1971) 23.
16. B. W. ROSEN and Z. HASIN, *Int. J. Eng. Sci.* **8** (1970) 157.
17. B. W. ROSEN, *Proc. Roy. Soc.* **A319** (1970) 79.
18. N. J. CHAMBERLAIN, unpublished report (1968).
19. S. DAS GUPTA, *Int. J. Solids Structures* **10** (1974) 1221.

Received 27 May and accepted 8 July 1977.